Computational Simulations of Implosions

Stephen Voelkel
Department of Aerospace and Mechanical Engineering, University of Notre Dame, IN 46556

UNIVERSITY OF NOTRE DAME
Center for Research Computing

Complex pattern formation created by implosion of Argon are predicted with the 2D Navier-Stokes equations using the wavelet adaptive mesh refinement (WAMR) technique. Upon removal of a diaphragm, collapsing flow structures interact with one another to produce complex, symmetrical patterns.

WAMR

WAMR adaptively discretizes with multiple levels of refinement to provide an accurate prediction to nonlinear partial differential equations at a computational cost that is independent of dimension[3]. The minimum Δx is related to the mean free path of molecular collisions[1].

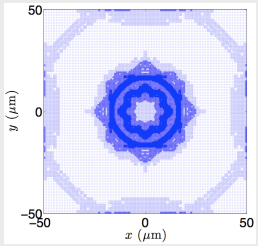

Figure 1. Grid distribution using WAMR with minimum Δx of 0.0031 μm for the octagonal diaphragm problem at a time of 80 ns.

WAMR was partially verified by comparing the predicted solution of a 1D Sod shock tube using Navier-Stokes equations with the exact solution to a Riemann problem as described by Sod[2].

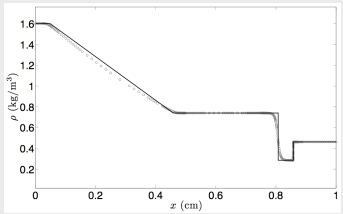

Figure 2. Density vs. position in a Sod shock tube with inert Argon initially at 300 K separated by a diaphragm with a high and low state initially at 1.0 atm and 0.1 atm, respectively.

Navier-Stokes Equations

$$
\begin{aligned}
\frac{\partial \rho}{\partial t} &= -\frac{\partial}{\partial x_i}(\rho u_i) \\
\frac{\partial}{\partial t}(\rho u_i) &= -\frac{\partial}{\partial x_j}(\rho u_j u_i) - \frac{\partial p}{\partial x_i} + \frac{\partial \tau_{ij}}{\partial x_j} \\
\frac{\partial}{\partial t}\left(\rho\left(e + \frac{1}{2}u_i u_i\right)\right) &= -\frac{\partial}{\partial x_j}\left(\rho u_j\left(\left(e + \frac{1}{2}u_i u_i\right) + \frac{p}{\rho}\right)\right) + \frac{\partial}{\partial x_i}(u_j \tau_{ji}) - \frac{\partial q_i}{\partial x_i} \\
p &= \rho R T \\
e &= c_v T \\
q_i &= -k\frac{\partial T}{\partial x_i} \\
\tau_{ij} &= \mu\left(\frac{\partial u_i}{\partial x_j} + \frac{\partial u_j}{\partial x_i}\right) - \frac{2}{3}\mu\delta_{ij}\frac{\partial u_k}{\partial x_k}
\end{aligned}
$$

Density Contours

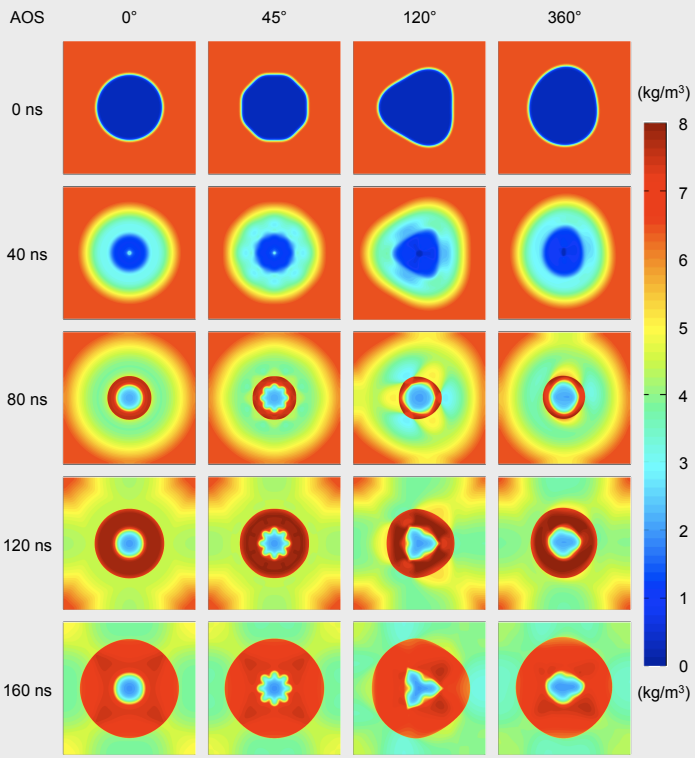

Figure 3. Density contours with an initial circular diaphragm, an octagonal diaphragm, a triangular diaphragm, and an asymmetric diaphragm (from left to right) at 40 ns time-intervals (from top to bottom).

Complex Pattern Formation

Symmetrical patterns were observed in imploding systems of Argon with an initial high and low pressure of 4.0 atm and 0.2 atm, respectively. Figure 3 shows the results for four different initial angles of symmetry (AOS). Initially, a shock and contact discontinuity collapse toward a central focal point until the shock fully collapses at approximately 40 ns. The compressed region explodes outward, crossing the contact discontinuity at approximately 60 ns. Complex, symmetrical patterns are further developed at the same angle of symmetry seen in the initial conditions. Symmetry breaks when the rarefaction wave begins to reflect from the boundary. These results are similar to those found by Wang *et al.*[4] using the Euler equations for imploding C_3H_8/air; the present results improve upon previous predictions with the inclusion of all diffusive terms.

Analysis

The temperature at the center ranges from six to eight times greater than T_o. As the angle of symmetry decreases, the peak, centerline temperature increases.

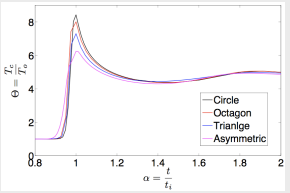

Figure 4. Non-dimensional temperature vs. non-dimensional time (scaled by the implosion time).

The number of collocation points used by WAMR dramatically increases as the reflected shock travels through the contact discontinuity. The overall complexity of the system is weakly dependent of the angle of symmetry.

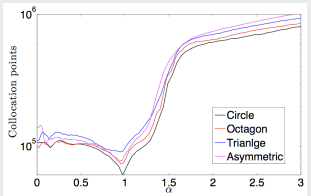

Figure 5. Collocation points used by WAMR vs. non-dimensional time for different initial conditions.

Figure 6 shows an *r-t* diagram depicting density contours. Evident is a shock front, a contact discontinuity, and a rarefaction fan. After the implosion, the shock explodes outward and passes through the contact discontinuity.

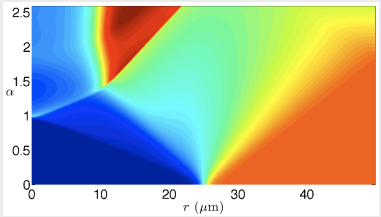

Figure 6. *r-t* diagram for an imploding structure (circular diaphragm).

References

1. J. M. Powers and S. Paolucci, *Accurate Spatial Resolution Estimates for Reactive Supersonic Flow with Detailed Chemistry*, AIAA Journal, Vol. 43, No. 5, May 2005.
2. G. A. Sod, *A Survey of Several Finite Difference Methods for Systems of Nonlinear Hyperbolic Conservation Laws*, Journal of Computational Physics, Vol. 27, pp. 1– 31, 1978.
3. O. V. Vasilyev and S. Paolucci, *A Fast Adaptive Wavelet Collocation Algorithm for Multidimensional PDEs*, Journal of Computational Physics, Vol. 138, pp. 16 – 56, 1997.
4. B. Wang, H. He, and S. T. J. Yu, Direct Calculation of Wave Implosion and Detonation Initiation, AIAA Journal, Vol. 43, No. 10, October 2005.

Acknowledgements

J. M. Powers • S. Paolucci • C. M. Romick • Z. Zikoski • NSF • CRC